Journal of Power Sources 185 (2008) 112–117

Contents lists available at ScienceDirect

Journal of Power Sources

journal homepage: www.elsevier.com/locate/jpowsour

Influence of cathode flow pulsation on performance of proton-exchange membrane fuel cell

Yun Ho Kim [a], Hun Sik Han [b], Seo Young Kim [c,*], Gwang Hoon Rhee [a]

[a] Department of Mechanical & Information Engineering, University of Seoul, Seoul 130-743, South Korea
[b] Department of Mechanical Engineering, Korea Advanced Institute of Science and Technology, Taejon 305-701, South Korea
[c] Energy Mechanics Research Center, Korea Institute of Science and Technology, Seoul 130-650, South Korea

ARTICLE INFO

Article history:
Received 24 March 2008
Received in revised form 23 May 2008
Accepted 6 June 2008
Available online 6 July 2008

Keywords:
Proton-exchange membrane fuel cell
Balance of plant
Cathode flow pulsation
Fuel cell efficiency
Power output

ABSTRACT

The effect of cathode flow pulsation on the performance of a 10-cell proton-exchange membrane fuel cell is investigated. An acoustic woofer generates a pulsating flow, which is added to a unidirectional flow supplied from a compressed air tank. By adding the flow pulsation, the fuel cell power output and the limit current dramatically increase while the fuel cell efficiency slightly decreases. As the pulsation amplitude increases, the improvement in fuel cell performance is more pronounced. The performance enhancement shows no obvious dependency on a pulsation frequency change from 10 to 30 Hz. The cathode flow pulsation effect is more distinct at low cathode flow rates.

1. Introduction

The proton-exchange membrane fuel cell (PEMFC) has received much attention as a promising candidate for future power generation. For this reason, considerable research and development efforts PEMFCs have been implemented [1–3]. It is known that both the configuration of the flow channels in bipolar plates and the membrane electrode assembly (MEA) significantly affect the fuel cell performance [4,5]. The performance of PEMFC is also influenced by thermo-fluidic parameters, such as the flow rates in the cathode and the anode, the humidity, the operating pressure and temperature.

To date, most of the research and development activities on PEMFCs have focused on the electrochemistry and, in particular, on the proton transport media [6,7]. By contrast, reported studies on balance-of-plant (BOP) are relatively small [8–10], although the BOP is essential to fuel cell operation. The optimum design of BOP is crucial to guarantee reliable operation and to minimize parasitic energy loss.

A PEMFC system consists of a fuel supply, an air supply, a water management system, a thermal management system, a power management system, and a fuel cell stack [11,12]. For the air supply, a blower or a compressor is generally used to feed air to the cathode flow channels in a stack. The air is supplied by a blower or a compressor passes through the cathode channels and is diffused through the gas-diffusion layer (GDL) for reaction. The performance of a fuel cell stack depends on the diffusion resistance in the GDL. For this reason, a blower or a compressor should provide a sufficient flow of air to overcome this resistance. On the other hand, an increase in the blowing capacity of air feeders results in an excessive parasitic power loss and increases the weight, volume and noise level of the system.

It has been well reported, both experimentally and numerically, that flow pulsation can increase the diffusion between two reservoirs that have a concentration gradient due to enhanced dispersion [13,14]. In fact, the diffusion is increased by up to three to four orders of magnitude above the molecular diffusion coefficient [13]. In this study, therefore, flow pulsation is adopted to enhance the uniformity of both oxygen and temperature distributions in the cathode flow channels. The flow pulsation is added to a unidirectional air flow supplied by a compressed air tank. By changing the frequency and the amplitude of the flow pulsation, the performance of a PEMFC is compared with that in the absence of flow pulsation.

2. Experiment methods and procedures

The experimental set-up for the performance measurement of a 10-cell PEMFC consisted of an air supply, a hydrogen supply,

* Corresponding author. Tel.: +82 2 958 5683; fax: +82 2 958 5689.
E-mail addresses: khhcp99@kaist.ac.kr (H.S. Han), seoykim@kist.re.kr (S.Y. Kim), ghrhee@uos.ac.kr (G.H. Rhee).

0378-7753/$ – see front matter © 2008 Elsevier B.V. All rights reserved.
doi:10.1016/j.jpowsour.2008.06.069

Nomenclature

D	depth of a cathode channel
L	length of a cathode channel
lpm	litres per minute
V_c	average voltage from a cell
V_{pp}	pulsation amplitude, peak-to-peak voltage to woofer
W	width of cathode channel

Greek letters

η	fuel cell efficiency based on higher heating value of hydrogen
μ_f	fuel utilization coefficient

a nitrogen supply, a temperature controller and a fuel cell stack, as shown in Fig. 1. Air was supplied from a compressed air tank through a rectangular Plexiglas duct where the flow pulsation was added. An 8 in.-woofer (Sammi, SR-08B100) was used to produce the flow pulsation. A function generator (HP-33120A) generated a sinusoidal signal with a specific frequency, and the signal was amplified by a signal amplifier. The amplified signal was sent to the woofer through a digital oscilloscope (LeCroy, LT342) to check the input frequency. The mean airflow rate was controlled by an MFC, and the air temperature and humidity were controlled by a heater and a humidifier. Compressed hydrogen of 99.999% purity was supplied to the anode, which was also controlled by an MFC. Several hydrogen flow rates were selected with fixed values of inlet humidity and temperature. A pressure regulator maintained the internal pressure of the stack at 1.5 bar [15].

An NP50 PEMFC stack (heliocentric Energiesysteme GmbH) consisting of 10 cells was employed. Each cell had 14 parallel and straight cathode channels of 1.93 mm (W) × 3.0 mm (D) × 70 mm (L) with ribs (W_L) of 1.7 mm width, as shown in Fig. 2. The active area of each cell was 25 cm^2 in square shape.

The following procedure was implemented to start-up and obtain polarization curves [15,16]. First, nitrogen was used to purge impurities inside the anode channel of the stack for 20 min. To activate the MEA inside the stack, air and hydrogen were supplied until a steady-state was reached for approximately 30 min under a current loading of 3 A. The cathode and anode humidities were set at 70 and 50%, respectively. After reaching a steady-state, the open-circuit voltage (OCV) was measured. The current loading was increased to a specific value by using an electric load (Daegil Electronics Co., EL-500P). The stack voltage was then measured again in a steady-state. Finally, the polarization curve was obtained for various current loadings.

After finishing the above experiments, the following procedure was undertaken to prevent any deterioration in the MEA from the remaining hydrogen. First, the external loading was removed and the hydrogen supply was shut off. Then the stack was purged with nitrogen. Simultaneously, the air supply was shut off. Finally, the stack was cooled under the action of the temperature control unit.

3. Results and discussion

3.1. Steady non-pulsating flow

The polarization and the power curves without flow pulsation are shown in Figs. 3–5. The inlet gas temperatures at the anode and the cathode are fixed at 50 and 33 °C, respectively. The relative humidities at the anode and the cathode are set at 50 and 70%, respectively. As the anode flow rate increases from 1 to 3 lpm at a fixed cathode flow rate of 30 lpm and a stack temperature of 50 °C the current limit and the fuel cell power decrease at a given voltage, see Fig. 3. Such a low performance of the stack with increasing hydrogen flow rates is attributed to increased dehydration of the proton-exchange membrane. The membrane dehydration increases the voltage losses due to a higher ohmic resistance when the stack is operated under conditions of relatively low humidity.

The effect of the cathode flow rate on the polarization and power curves for the steady flow condition is shown in Fig. 4. As the air flow rate increases from 10 to 30 lpm at a fixed anode flow rate of 1 lpm and a stack temperature of 50 °C, the stack performance is dramatically enhanced. When the air flow rate is low, the oxygen supply to the membrane decreases as the air reaches the end of the cathode channel [17]. In addition, the low air flow rate results in a reduced capability of water removal in the cathode channels at high current loading.

As the stack temperature increases from 50 to 70 °C, the stack performance obviously decreases, see Fig. 5. Conversely, it is generally known that as the stack temperature increases the PEM fuel cell

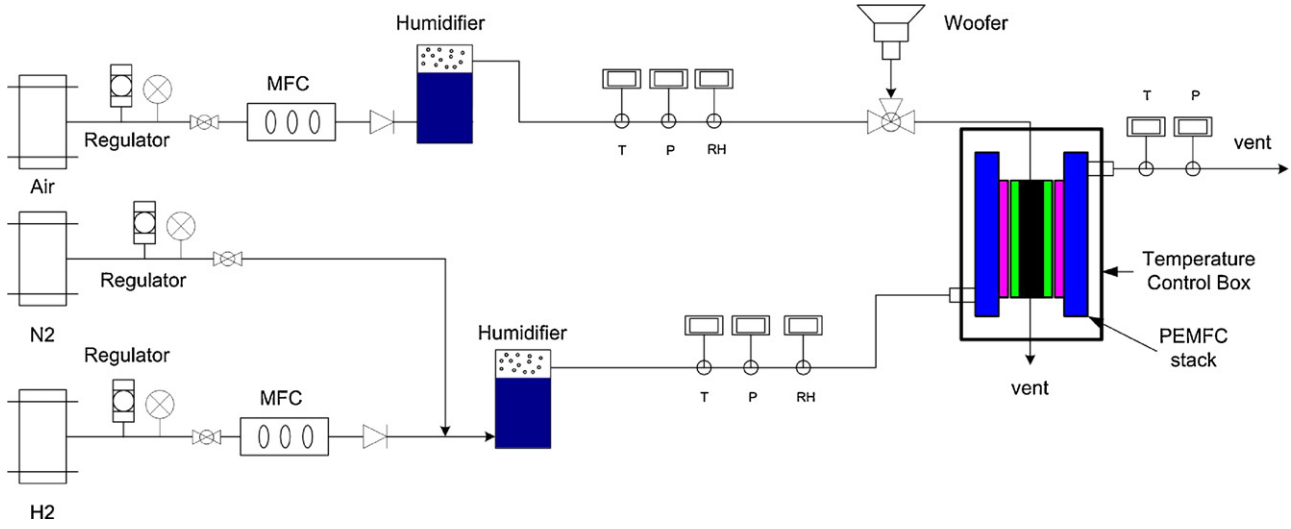

Fig. 1. Schematic diagram of experimental set-up.

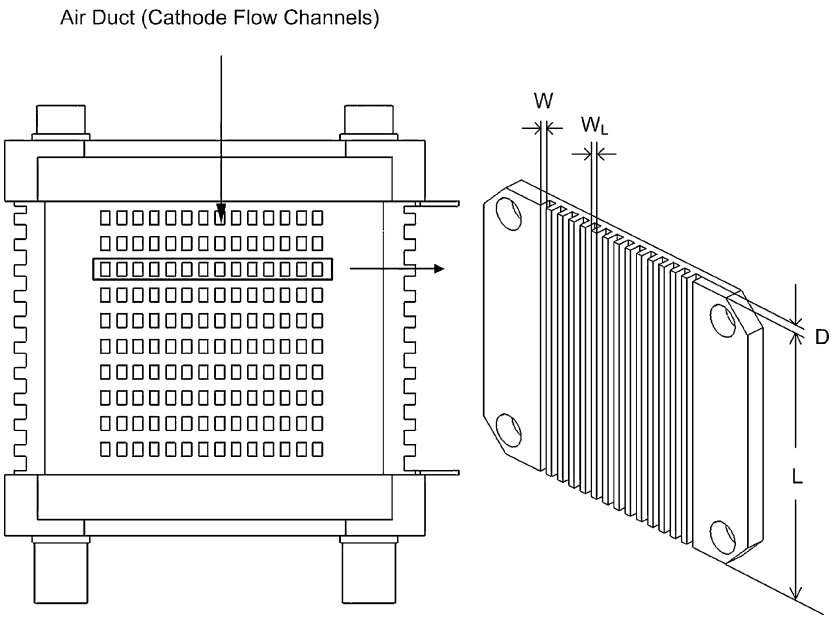

Fig. 2. Cathode channel configuration of NP50 PEMFC stack.

performance increases until the operating temperature increases over 90 °C. As the stack temperature increases at low humidity, however, the cathode and anode inlet gases are unable to humidify the membrane effectively but take water away from the membrane [18], which reduces the active sites. Consequently, the fuel cell stack performance can decrease.

3.2. Cathode pulsating flow

For the cathode flow pulsation experiments in this study, the anode flow rate, the stack operating temperature and the humidity are fixed at 1 lpm, 50 °C and 50%, respectively. The time-averaged cathode air flow rate varies from 10 to 30 lpm.

The polarization and power curves according to various cathode pulsation frequencies and amplitudes are displayed in Figs. 6 and 7. In Fig. 6, when the steady non-pulsating air flow is supplied to the cathode flow channels, the maximum power output reaches approximately 34 W at 7 A loading. As the flow pulsation is added

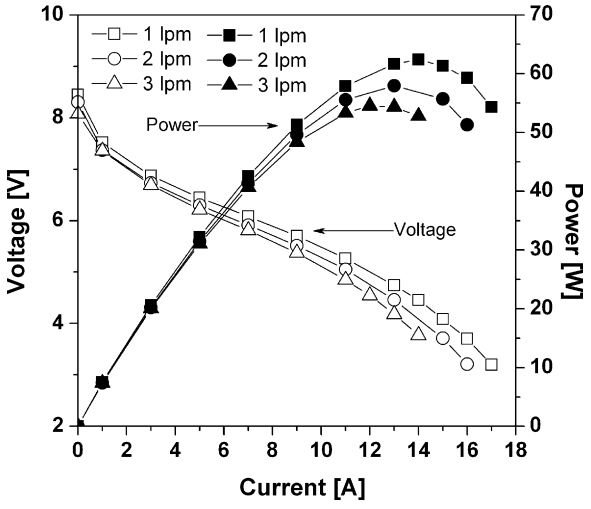

Fig. 3. Effect of anode flow rate on polarization and power curves. Cathode flow rate is 30 lpm.

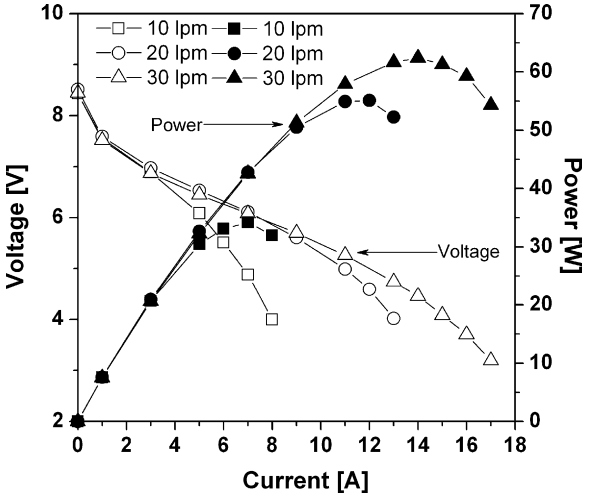

Fig. 4. Effect of cathode flow rate on polarization and power curves. Anode flow rate is 1 lpm.

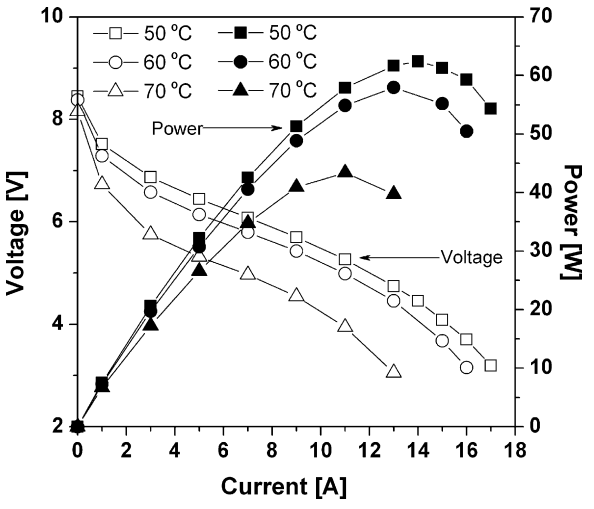

Fig. 5. Effect of stack temperature on polarization and power curves. Anode and cathode flow rates are 1 and 30 lpm.

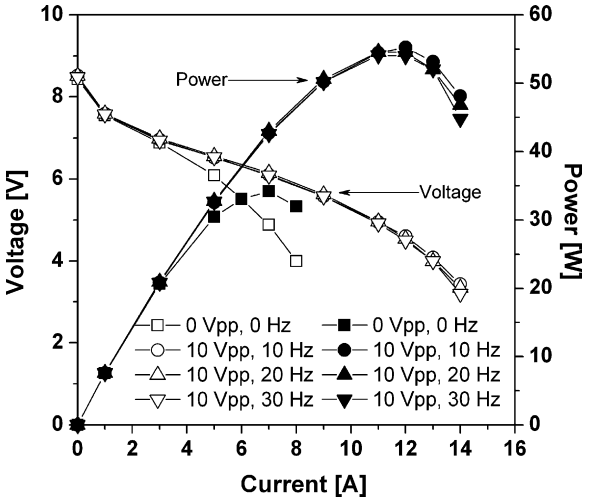

Fig. 6. Polarization and power curves according to pulsation frequency when anode and cathode flow rates are 1 and 30 lpm, respectively.

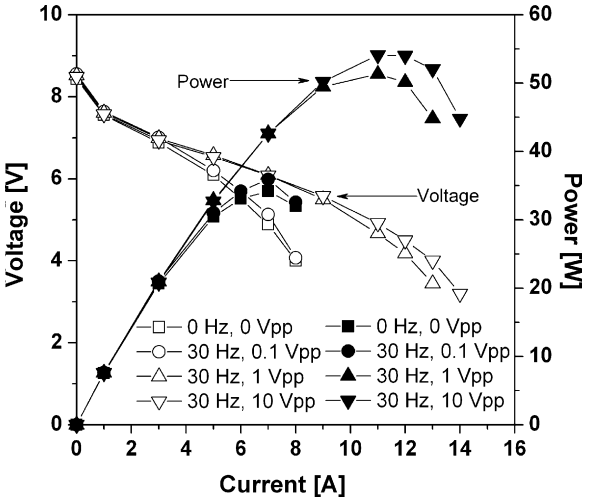

Fig. 7. Polarization and power curves according to pulsation amplitude when anode and cathode flow rates are 1 and 30 lpm, respectively.

to the cathode, however, the maximum power output dramatically increases to 55 W at 12 A loading. It is noted that such a dramatic enhancement in fuel cell performance caused by the flow pulsation is little changed for the frequency variation in the range considered in this study. As seen in the polarization curve of Fig. 6, the enhancement of output voltage by the cathode flow pulsation is negligible at a low current loading. As the current loading increases beyond 3 A, however, the cathode flow pulsation signif-

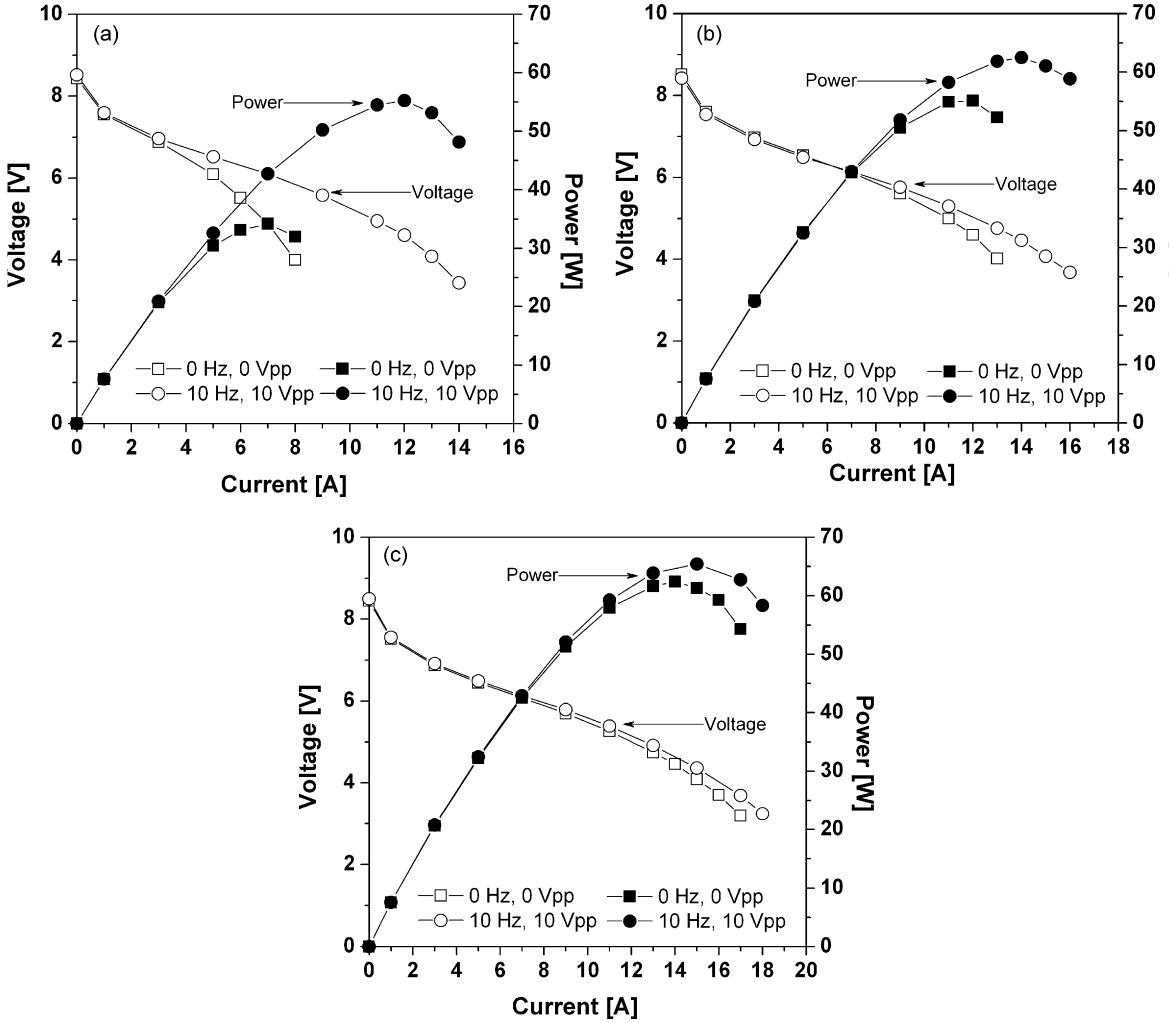

Fig. 8. Polarization and power curves for various cathode flow rates at an anode flow rate of 1 lpm: (a) 10 lpm, (b) 20 lpm and (c) 30 lpm.

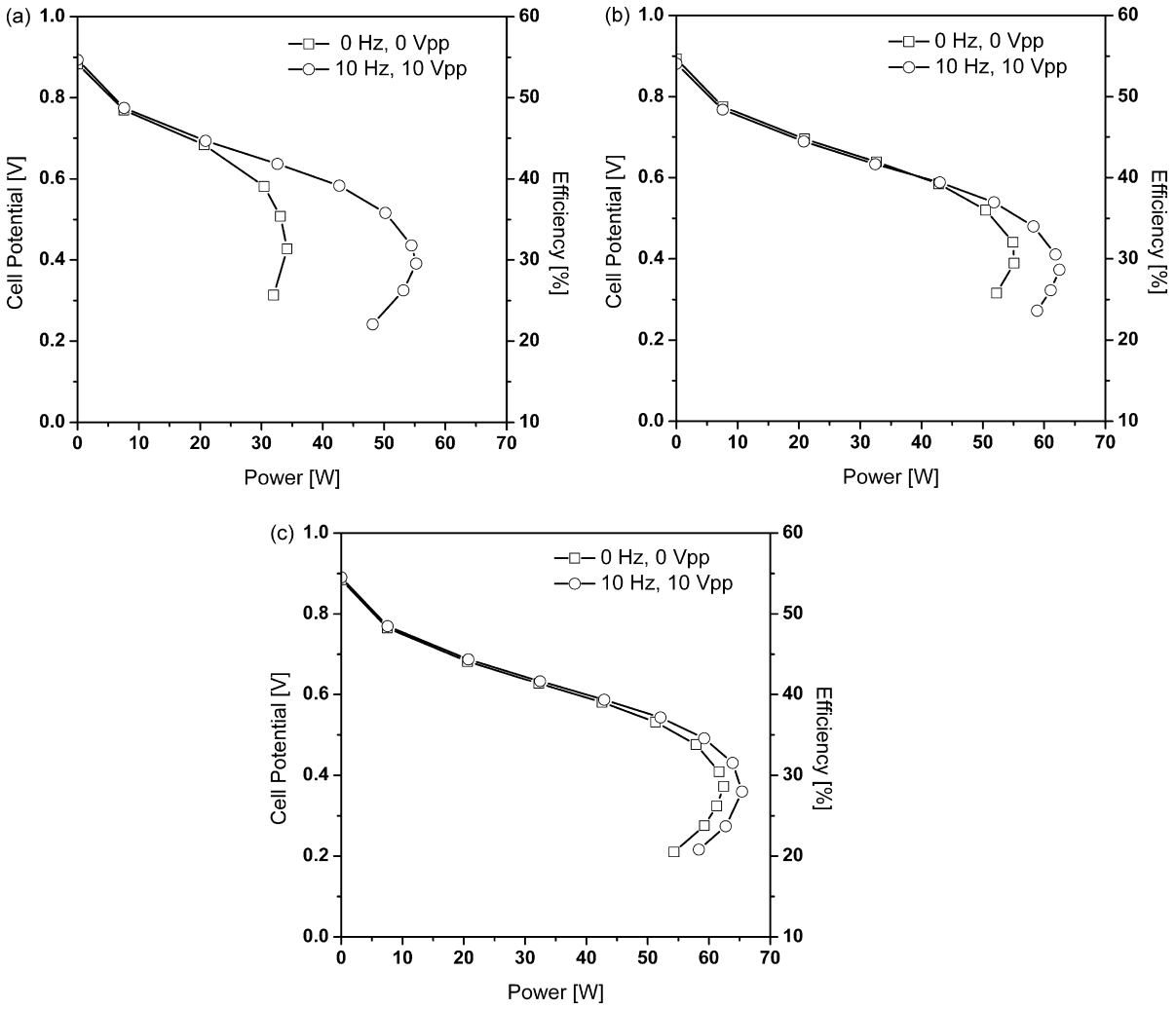

Fig. 9. Fuel cell efficiency for various cathode flow rates at an anode flow rate of 1 lpm: (a) 10 lpm, (b) 20 lpm and (c) 30 lpm.

icantly increases the output voltage and extends the current limit from 8 A for steady non-pulsating cathode flow to 14 A for cathode flow pulsation.

The current limit and power output are enhanced as the amplitude increases from 0.1 to 10 V_{pp} at a fixed pulsation frequency of 30 Hz, as shown in Fig. 7. Therefore, cathode flow pulsation obviously augments fuel cell performance. This effect is attributed to enhanced dispersion by the flow pulsation. Jaeger and Kurzweg [19] showed that the dispersion under a pulsating flow was more effective than that in a steady turbulent flow such that the diffusion coefficient could be significantly increased. Therefore, the oxygen distribution, as well as the temperature distribution, inside the cathode channels can be improved by enhanced diffusion to yield an improvement in fuel cell performance.

Polarization and power curves at several cathode flow rates are presented in Fig. 8. The pulsation frequency is 10 Hz and the amplitude is 10 V_{pp}. The effect of flow pulsation is more pronounced at low flow rates. The impact of cathode flow pulsation decreases as the flow rate increases. It should be noted in Fig. 8(a) and (b) that the power output with the cathode flow pulsation at a flow rate of 10 lpm is almost equal to the power output for a steady non-pulsating cathode flow at 20 lpm. The flow pulsation results in 62, 13 and 5% increments of the maximum power output when the cathode flow rates are 10, 20 and 30 lpm, respectively.

3.3. Fuel cell efficiency

The fuel cell efficiency based on the higher heating value (HHV) of hydrogen is given by [20]:

$$\eta = \mu_f \frac{V_c}{1.48} \times 100 \quad (1)$$

where V_c is the average cell voltage and μ_f is the fuel utilization coefficient defined as the ratio of the mass of fuel that has reacted to the mass of fuel input to a cell. A good estimate is 0.95.

The fuel cell efficiency as a function of power output at a pulsation frequency of 10 Hz and an amplitude of 10 V_{pp} is presented in Fig. 9. As displayed in Fig. 9(a), a maximum power of 34 W can be achieved at an efficiency of 31% for a steady non-pulsating flow rate of 10 lpm. Cathode flow pulsation raises the maximum power to 55 W at an efficiency of 29%. Therefore, a 62% enhancement in maximum power can be obtained at a slightly reduced efficiency by adopting cathode flow pulsation. Even at the same efficiency, it is noted that the fuel cell power output substantially increases with cathode flow pulsation. The fuel cell efficiency at a cathode flow rate of 20 lpm is given in Fig. 9(b). The maximum power output is 55 W for a steady non-pulsating flow and 62 W with cathode flow pulsation. The corresponding fuel cell efficiencies are 29.5 and 28.6%. For a cathode flow rate of 30 lpm, the maximum power out-

puts are 62 and 65 W at efficiencies of 28.6 and 28% for steady and pulsating flow operations, respectively. As the steady cathode flow rate increases, therefore, enhancement of the maximum power by flow pulsation slows. The fuel cell efficiency decreases slightly with increase of the cathode flow rate. Consequently, it will be more efficient to use cathode flow pulsation at low cathode flow rates. Cathode flow pulsation can reduce blower power, as well as the volume, weight and noise of fuel cell systems.

4. Conclusion

The present study has investigated the effects of cathode flow pulsation on the overall performance of a 10-cell PEMFC with straight cathode flow channels. From the present flow pulsation experiments, the following conclusions can be drawn:

(1) The cell voltage, current limit and power output of fuel cell all dramatically increase by applying flow pulsation to the cathode channels.
(2) The enhancement in current limit and power output is pronounced as the pulsation amplitude is increased, but there is no obvious dependence on the flow pulsation frequency.
(3) Flow pulsation has a strong impact at low cathode flow rates. For instance, the maximum power increases by 62, 13 and 5% when the cathode flow rate is 10, 20 and 30 lpm, respectively.
(4) As the steady cathode flow rate is increased, the fuel cell efficiency, at which the maximum power could be achieved, is reduced. With cathode flow pulsation, the fuel cell efficiency decreases slightly compared with that without flow pulsation.

Acknowledgement

This work was supported by the research grant no. 2E19910 of Korea Institute of Science and Technology, Seoul, South Korea.

References

[1] M. Cappadonia, J.W. Erining, S.M.S. Niaki, U. Stimming, Solid State Ionics 77 (1995) 65–69.
[2] L.R. Jordan, A.K. Shukla, T. Behrsing, N.R. Avery, B.C. Muddle, M. Forsyth, J. Power Sources 86 (2000) 250–254.
[3] P. Sridhar, R. Perumal, B. RAjalakshmi, M. Raja, K.S. Dhathathreyan, J. Power Sources 101 (2001) 72–78.
[4] M. Noponen, T. Mennola, M. Mikkola, T. Hottinen, P. Lund, J. Power Sources 106 (2002) 304–312.
[5] S. Dutta, S. Shimpalee, J.W. Van Zee, J. Heat Mass Transfer 44 (2001) 2029–2042.
[6] W. Vielstich, A. Lamm, H. Gasteiger, Handbook of Fuel Cells, vol. 3, Wiley, New York, 2003 (Part 3).
[7] H.-S. Chu, F. Tsau, Y.-Y. Yan, K.-L. Chen, J. Power Sources 176 (2008) 499–514.
[8] M. Lin, Y. Cheng, M. Lin, S. Yen, J. Power Sources 140 (2005) 346–349.
[9] M. Oszcipok, M. Zedda, J. Hesselmann, M. Huppmann, M. Wodirch, M. Junghardt, C. Hebling, J. Power Sources 157 (2006) 666–673.
[10] U.S. Selamogullari, T.R. Willemnain, D.A. Torrey, J. Power Sources 171 (2007) 805–810.
[11] J.H. Hirschenhorer, D.B. Stauffer, R.R. Engleman, M.G. Klett, Fuel Cell Handbook, 4th ed., Parsons Corporation, Pennsylvania, 1998 (for the U.S. Department of Energy).
[12] W. Colella, J. Power Sources 106 (2002) 388–396.
[13] U.H. Kurzsweq, L. de Zhao, Phys. Fluids 27 (1984) 2624–2627.
[14] U.H. Kurzweq, J. Fluid Mech. 156 (1985) 291–300.
[15] Operating Instructions, NP50 Fuel Cell Stack, heliocentris Energiesysteme GmbH, Berlin, 2000.
[16] S.Y. Kim, W.N. Kim, J. Power Sources 166 (2007) 430–434.
[17] Q. Yan, H. Toghiani, H. Causey, J. Power Sources 161 (2006) 492–502.
[18] W.-M. Yan, C.-Y. Chen, S.-Y. Mei, C.-Y. Soong, F. Chen, J. Power Sources 162 (2006) 1157–1164.
[19] M.J. Jaeger, U.H. Kurzweg, Phys. Fluids 26 (1983) 1380–1382.
[20] J. Larminie, A. Dicks, Fuel Cell Systems Explained, John Wiley & Sons Ltd., 2003.